Journal of Visualized Experiments

An in vitro system to gauge the thrombolytic efficacy of histotripsy and a lytic drug

--Manuscript Draft--

Article Type:	Invited Methods Article - JoVE Produced Video
Manuscript Number:	JoVE62133R1
Full Title:	An in vitro system to gauge the thrombolytic efficacy of histotripsy and a lytic drug
Corresponding Author:	Aarushi Bhargava, Ph.D. UChicago Medicine Chicago, Illinois UNITED STATES
Corresponding Author's Institution:	UChicago Medicine
Corresponding Author E-Mail:	aarushib@uchicago.edu
Order of Authors:	Aarushi Bhargava, Ph.D.
	Samuel Hendley
	Kenneth Bader
Additional Information:	
Question	**Response**
Please specify the section of the submitted manuscript.	Bioengineering
Please indicate whether this article will be Standard Access or Open Access.	Standard Access (US$2,400)
Please indicate the **city, state/province, and country** where this article will be **filmed**. Please do not use abbreviations.	Chicago, Illinois, United States
Please confirm that you have read and agree to the terms and conditions of the author license agreement that applies below:	I agree to the Author License Agreement
Please provide any comments to the journal here.	

TITLE:

An In Vitro System to Gauge the Thrombolytic Efficacy of Histotripsy and a Lytic Drug

AUTHORS AND AFFILIATIONS:

Aarushi Bhargava[1], Samuel A. Hendley[2], Kenneth B. Bader[1,2]

[1]Department of Radiology, University of Chicago, Chicago, IL, USA
[2] Graduate Program in Medical Physics, University of Chicago, Chicago, IL, USA

Email addresses of co-authors:
Kenneth B. Bader (baderk@uchicago.edu)
Samuel A. Hendley (hendley@uchicago.edu)
Aarushi Bhargava (aarushib@uchicago.edu)

Corresponding author:
Aarushi Bhargava (aarushib@uchicago.edu)

KEYWORDS:

histotripsy, lysotripsy, thrombolysis, hemolysis, deep vein thrombosis, passive cavitation imaging, focused ultrasound, acoustic cavitation

SUMMARY:

Histotripsy-aided lytic delivery or lysotripsy is under development for the treatment of deep vein thrombosis. An in vitro procedure is presented here to assess the efficacy of this combination therapy. Key protocols for the clot model, image guidance, and assessment of treatment efficacy are discussed.

ABSTRACT:

Deep vein thrombosis (DVT) is a global health concern. The primary approach to achieve vessel recanalization for critical obstructions is catheter-directed thrombolytics (CDT). To mitigate caustic side effects and the long treatment time associated with CDT, adjuvant and alternative approaches are under development. One such approach is histotripsy, a focused ultrasound therapy to ablate tissue via bubble cloud nucleation. Pre-clinical studies have demonstrated strong synergy between histotripsy and thrombolytics for clot degradation. This report outlines a benchtop method to assess the efficacy of histotripsy-aided thrombolytic therapy or lysotripsy.

Clots manufactured from fresh human venous blood were introduced into a flow channel whose dimensions and acousto-mechanical properties mimic an iliofemoral vein. The channel was perfused with plasma and the lytic, recombinant tissue-type plasminogen activator. Bubble clouds were generated in the clot with a focused source designed for the treatment of femoral venous clots. Motorized positioners were used to translate the source focus along the clot length. At each insonation location, acoustic emissions from bubble cloud were passively recorded, and beamformed to generate passive cavitation images. Metrics to gauge treatment efficacy included clot mass loss (overall treatment efficacy), and the concentration of D-dimer (fibrinolysis) and

hemoglobin (hemolysis) in the perfusate. There are limitations to this in vitro design, including lack of means to assess in vivo side effects or dynamic changes in flow rate as the clot lyses. Overall, the setup provides an effective method to assess the efficacy of histotripsy-based strategies to treat DVT.

INTRODUCTION:

Thrombosis is the condition of clot formation in an otherwise healthy blood vessel that obstructs circulation[1,2]. Venous thromboembolism has an annual healthcare cost of $7–10 billion, with 375,000–425,000 cases in the United States[3]. Pulmonary embolism is the obstruction of the pulmonary artery and is the most serious consequence of venous thromboembolism. The primary source of pulmonary obstruction is deep vein thrombi, primarily from iliofemoral venous segments[4–6]. Deep vein thrombosis (DVT) has inherent sequela besides pulmonary obstructions, with long term complications that result in pain, swelling, leg ulcerations, and limb amputations[7–9]. For critical obstructions, catheter directed thrombolytics (CDT) are the frontline approach for vessel recanalization[10]. The outcome of CDT depends on a number of factors, including thrombus age, location, size, composition, etiology, and patient risk category[11]. Moreover, CDT is associated with vascular damage, infections, bleeding complications, and long treatment time[10]. Next generation devices aim to combine mechanical thrombectomy with thrombolytics (i.e., pharmacomechanical thrombectomy)[12,13]. Use of these devices lower the lytic dosage leading to reduced bleeding complications, and shortened treatment time[12–14] as compared to CDT. These devices still retain issues of hemorrhagic side-effects and incomplete removal of chronic thrombi[15]. An adjuvant strategy is thus needed that can remove the thrombus completely with lower bleeding complications.

One potential approach is histotripsy-aided thrombolytic treatment, referred to as lysotripsy. Histotripsy is a non-invasive treatment modality that uses focused ultrasound to nucleate bubble cloud in tissues[16]. Bubble activity is generated not via exogenous nuclei, but by the application of ultrasound pulses with sufficient tension to activate nuclei intrinsic to tissues, including clot[17,18]. The mechanical oscillation of the bubble cloud imparts strain to the clot, disintegrating the structure into acellular debris[19]. Histotripsy bubble activity provides effective degradation of retracted and unretracted blood clots both in vivo and in vitro[20–22]. Prior studies have[23,24] demonstrated that the combination of histotripsy and the lytic, recombinant tissue-type plasminogen activator (rt-PA), significantly increases treatment efficacy compared to lytic alone or histotripsy alone. It is hypothesized that two primary mechanisms associated with histotripsy bubble activity are responsible for the improved treatment efficacy: 1) increased fibrinolysis due to enhanced lytic delivery, and 2) hemolysis of red blood cells within the clot. The bulk of the clot mass comprises red blood cells[24], and, therefore, tracking erythrocyte degradation is a good surrogate forablation of the sample. Other formed clot elements are also likely disintegrated under histotripsy bubble activity but are not considered in this study.

Here, a benchtop approach to treat DVT in vitro with lysotripsy is outlined. The protocol describes critical operating parameters of the histotripsy source, assessment of treatment efficacy, and image guidance. The protocol includes designing a flow channel to mimic an iliofemoral venous segment and manufacturing human whole blood clots. The experimental procedure outlines the

positioning of the histotripsy source and imaging array to achieve histotripsy exposure along the clot placed in the flow channel. Relevant insonation parameters to attain clot disruption and minimize off-target bubble activity are defined. The use of ultrasound imaging for guidance and assessment of bubble activity is illustrated[24]. Metrics to quantify treatment efficacy such as clot mass loss, D-dimer (fibrinolysis), and hemoglobin (hemolysis) are outlined[23–27]. Overall, the study provides an effective means for executing and assessing the efficacy of histotripsy-based strategies to treat DVT.

PROTOCOL:

For the results presented here, venous human blood was drawn to form clots after approval from the local internal review board (IRB #139-1300) and written informed consent provided by volunteer donors[24]. This section proposes a design protocol for lysotripsy of thrombus. The protocol is based on a previous work by Bollen et al.[24].

1. Clot modeling

NOTE: Prepare the clots within 2 weeks prior to the day of the experiment to ensure clot stability and maximize retraction[28]. Prepare the clot following the approval from local institutional review board.

1.1. Prepare borosilicate Pasteur pipette for storing the blood (see **Table of Materials** for specifications of the pipette). Borosilicate tubes are used because of the hydrophilic nature of the material which promotes platelet activation and clot retraction[29]. Seal the tip of the pipette via heating over a Bunsen burner.

1.2. Draw fresh human venous blood. Aliquot the total blood drawn in 2 mL increments per desired clot. Transfer each 2 mL aliquot to one Pasteur pipette.

NOTE: Execute step 1.2 within approximately 3 min so that blood does not clot before transferring to pipettes.

1.3. Incubate the blood aliquots within the pipettes (equal to the number of clots required) in a water bath for 3 h at 37 °C.

1.4. Store the pipettes for a minimum of 3 days at 4 °C to allow for retraction of clots[28]. As the clots retract, serum will be observed to accumulate within the pipette. The rt-PA response of clots remains stable for 2 weeks following formation[28].

2. Water tank preparation

2.1. Fill the water tank with reverse osmosis water. Line the bottom surface of the tank with an acoustic absorbing material to reduce reflection of the therapy or imaging ultrasound pulses. Use a water handling system to degas and filter the water to minimize bubble nuclei.

NOTE: One way to filter the water is using a filter bag. The specifications of the bag used for generating the representative results is given in the **Table of Materials**.

2.2. Place two heating elements at the bottom surface of the tank. Heat the water to 37.3 ˚C to achieve the maximum lytic enzymatic activity[30].

2.3. Setup a flow channel as shown in **Figure 1A**. The flow channel consists of tubing, a model vessel with material and geometric properties representative of an iliofemoral vein, a reservoir for plasma, and a syringe on the distal most end of the reservoir (**Table of Materials**). The syringe is connected to a pump to regulate a flow through the channel during the experiment.

2.4. Manually submerge the flow channel in the water tank to bring the channel to physiologic temperature during the degassing/filtering/heating stage (steps 2.1 and 2.2).

3. Preparation of plasma and rt-PA mixture

3.1. Prior to experiment day

NOTE: When stored at -80 °C, plasma is stable for at least 2.5 years[31] and rt-PA is stable for at least 7 years[32]. Therefore, execute step 3.1 anytime within these periods to ensure stability of the two components.

3.1.1. Dilute the rt-PA obtained from a manufacturer in powdered form to 1 mg/mL in sterile water.

3.1.2. Aliquot 100 µL of diluted rt-PA into 0.5 mL centrifuge tubes and store them at -80 °C.

3.1.3. Aliquot 35 mL of human fresh-frozen type O plasma in 50 mL centrifuge tubes. Store the tubes at -80 °C.

3.2. On the experiment day

3.2.1. Retrieve plasma aliquots from the freezer. Retrieve as many aliquots as the number of clots to be tested that day. Immerse the frozen aliquots in a water bath at 37 °C to thaw (~10 min).

3.2.2. Once plasma has thawed, pour into a beaker that is triply rinsed with ultrapure water. Lightly cover the mouth of the beaker with aluminum foil to prevent contamination and place the beaker in the water bath. Allow the foil to be loose enough to allow air to contact the plasma.

3.2.3. Let plasma equilibrate at 37 °C to atmospheric pressure for at least 2 h.

3.2.4. Take out the frozen rt-PA vials and place on ice until needed, with one vial for each experiment run.

3.2.5. Make low gelling agarose (2%) in a 50 mL flask, by dissolving agarose in ultrapure water. Choose the total amount of agarose solution such that approximately 2 mL is available for each specimen to be analyzed. Heat the solution in flask in a microwave until bubbly. Secure the flask with a waterproof screw lid on it. Submerge the flask in the water bath alongside the plasma.

NOTE: This step ensures agarose is available to secure exposed clot segments for histology analysis following histotripsy insonation.

4. Setting up histotripsy source and imaging array

4.1. Ensure the motorized positioners can be controlled from the runtime environment of a programming platform, using directions and commands provided by the manufacturer. Check that the motors of the system are connected to the appropriate port of the computer with the runtime environment.

4.2. Mount the histotripsy source on the motorized positioning system as shown in **Figure 1B**.

4.3. Connect the histotripsy source to its driving electronics (e.g., power amplifier and function generator) via the appropriate connectors (e.g., BNC cables) as specified by the manufacturer.

NOTE: Ensure that the driving electronics of the histotripsy source can be controlled via the runtime environment.

4.4. Cover the imaging array with a probe cover and affix the array coaxially in the aperture of the histotripsy source as shown in **Figure 2**. Be sure to understand the orientation of the imaging plane relative to the orientation of the histotripsy source.

4.5. Connect the imaging array to an ultrasound scanning system. Ensure that this system can control the operation and triggering of the imaging array, and collect imaging data, as per the commands provided by the manufacturer of the scanner.

4.6. Submerge the histotripsy source/imaging array into the tank while degassing as shown in **Figure 1A**. Gently remove any air bubbles using a syringe from the surface of the histotripsy source or imaging array.

NOTE: Immerse the histotripsy source and imaging array completely in water before operation. Avoid touching the surface of the histotripsy source.

4.7. Acquire B-mode images at a rate of 20 frames per second using the imaging array and the built-in commands of the scanner. Adjust the imaging window to ensure visualization of the focus of the histotripsy source in these real-time images.

NOTE: It is assumed that the dimensions of the focal region of the acoustic field are known.

4.8. Set the operating parameters of the histotripsy source, including fundamental frequency (e.g., 1.5 MHz), pulse repetition frequency (e.g., 20–100 Hz), pulse duration (e.g., 1–20 cycles per pulse), and total number of pulses per location (e.g., 100–2,000)[18,23,24,33]. Modify these parameters if sufficient clot lysis is not achieved or if the bubble activity extends beyond the lumen of the model vessel. To set these parameters, use the protocol provided by the manufacturer of the source or use a programming platform that can communicate with the source.

4.9. Using the manufacturer's protocol or programming platform used in step 4.8, run the histotripsy source at the set parameters in degassed water only, without any obstruction in the surrounding environment. Increase the voltage applied to the histotripsy source until a bubble cloud is formed.

4.10. Using the real-time imaging of step 4.7, adjust the position of the imaging array inside the confocal transducer opening until the bubble cloud is located approximately at the center of the image window. The bubble cloud is the region of hyperechoic pixels in the imaging plane (**Figure 3**). Tighten the screws to hold the imaging array firmly in the transducer opening.

NOTE: If the array is aligned properly, the azimuthal position of the bubble cloud should be approximately at 0 mm. The imaging array may project slightly from the inner surface of the therapy source, and therefore the range position of the bubble cloud may differ from the focal length of the source.

4.11. Identify the bubble cloud location in the imaging plane. Assign the focus of the histotripsy source as the center of the bubble cloud (**Figure 3**).

4.12. Record the detected focal location (step 4.11) in the imaging window (**Figure 3**). A possible way to mark the focal position is placing a cursor to note the location in the imaging window, if available with the imaging platform.

4.13. Discontinue insonation and set the voltage applied to the histotripsy source to 0 V.

5. Clot preparation

5.1. Remove the clot from the pipette by cutting the sealed end with pliers. Let the clot slide into a Petri dish along with the serum. If the clot does not dislodge, gently apply pressure from the other end of the pipette via saline flush to remove the clot.

5.2. Cut the clot to 1 cm length using a scalpel, aiming for a uniform piece from the center (i.e., away from sections of the clot formed at the top or bottom of the pipette).

5.3. Use a cleaning wipe to blot the cut section of the clot gently to remove excess fluid.

5.4. Using tweezers, place the clot section gently on a weighing scale and record the weight.

5.5. Manually raise the flow channel out of the water tank and remove the model vessel from the flow channel.

5.6. Place the clot in the model vessel using tweezers and attach the model vessel again to the flow channel.

NOTE: A nylon rod can be placed within the model vessel to prevent the clot from moving downstream due to the flow.

5.7. Lower the flow channel into the tank in such a way that the proximal end of the stage relative to the reservoir is low compared to the distal side. The angling of the stage in this manner prevents trapping of bubbles in the model vessel when plasma is drawn through the flow channel in step 6.1.

5.8. Add 30 mL of plasma to the reservoir using a pipette and monitor the temperature until it reaches at least 36 °C.

5.9. Use a pipette to dispense the rt-PA (80.4 µg in 30 mL of plasma, 2.68 µg/mL) into the plasma reservoir. Stir the plasma with the pipette to ensure a uniform rt-PA distribution within the reservoir.

6. Priming the flow channel

6.1. Draw plasma into the flow channel from the reservoir via the syringe pump until the plasma fills the model vessel. This rate does not disturb the clot but fills the model vessel efficiently.

NOTE: If the clot is not flush with the nylon rod, use short pump draws at 60 mL/min to try to force the plasma downstream the clot or manually draw the syringe. Limit the amount of plasma drawn in this process or refill the reservoir using additional plasma/rt-PA to ensure 30 mL of solution in the flow channel.

6.2. Using the motorized positioners, align the imaging array parallel to the length of the clot using the imaging script (step 4.7). The parallel alignment enables the user to visually ensure proper placement of the clot and absence of bubbles inside the model vessel.

6.3. Level the model vessel manually and visually ensure that no air bubbles are present using the imaging window (step 4.7).

7. Experiment procedure

7.1. Pre-treatment

NOTE: This step is to plan a path for the histotripsy source/imaging array for uniform histotripsy exposure along clot length.

7.1.1. Align the imaging array using the motorized positioners such that the imaging plane is parallel to the cross-section of the clot (i.e., perpendicular to the orientation described in step 6.2).

7.1.2. Under guidance via the imaging window (step 4.7), move the histotripsy source to the proximal end of the clot relative to the reservoir using the motorized positioners. At this point, adjust the histotripsy source position such that the marked focal point in step 4.12 aligns with the center of the clot.

7.1.3. Determine the insonation path along the clot length. To define this path, set three waypoints along the length of the clot (i.e., positions of the motors where histotripsy bubble activity is contained within the clot) in 5 mm increments. Align the waypoints such that the overall motion of the histotripsy source along the path is antegrade with flow in the system (i.e., the first waypoint is at the most proximal end of the clot relative to the reservoir, and the third waypoint is in the distal position relative to the reservoir).

7.1.4. Prior to finalizing each waypoint, fire test pulses from the histotripsy source with the same insonation parameters as step 4.8 but reduce the overall exposure to 10 total pulses. Adjust the position of the histotripsy source using the motorized positioners if necessary, to contain bubble activity within the clot.

7.1.5. At each waypoint, save the motor positions using the commands provided by the manufacturer, similar to the step 4.1.

7.2. Treatment

NOTE: This step defines the procedure to treat the clot along its length according to the path defined in the pre-treatment step.

7.2.1. Run the syringe pump at 0.65 mL/min and wait for meniscus of the plasma to move. This flow rate mimics a near total occlusion of the iliofemoral vasculature[24,34].

7.2.2. Interpolate the path created in step 7.1.3 with intermediate steps between the established waypoints with a fixed step size (e.g., 0.5 mm). The step size is chosen to be smaller than half the width of the focal region as measured along the clot length (elevational direction of the imaging array). Move the histotripsy source using motorized positioners at each path location with insonation parameters defined in step 4.8.

7.2.3. Monitor/image bubble activity during application of the histotripsy pulse at each path location using the imaging window (step 4.7). Center the image on the histotripsy focus with the

image dimensions covering 15 mm in the azimuth and range. Prior to the application of histotripsy pulse at each location, acquire a B-mode image to provide visualization of the clot and model vessel, by creating a script in a programming platform. Ensure the script establishes communication with the scanner using the manufacturer's commands.

7.2.4. During the application of the histotripsy pulse, implement the acquisition of acoustic emissions in the script in step 7.2.3 to form passive cavitation images post hoc[35]. Acquire one passive cavitation image after every 10 treatment pulses. Apply a flat time gain compensation of 50 at 8 incremental depths till the end of the imaging depth. Choose an appropriate acquisition window size such that the entire signal from the clot is captured with minimum loss of energy due to windowing[35].

7.2.5. If off-target bubble clouds are present, adjust the transducer position in situ with the motorized positioners.

NOTE: Monitor for missed triggers. Adjust the number of acquired imaging data sets to ensure the storage of data is completed before subsequent triggering.

8. Post experiment procedure

8.1. Manually raise the model vessel out of the water tank to drain the perfusate via gravity. Be sure to keep the flow channel levelled to prevent the clot from moving downstream and out of the model vessel during draining.

8.2. Collect the entire perfusate for further analysis in a small beaker (**Figure 4A**) by drawing plasma solution from the flow channel through the syringe pump.

8.3. Disconnect the model vessel and remove the clot. If necessary, inject a small amount of saline into the model vessel to gently dislodge the clot.

8.4. Wipe the clot similar to step 1.2.3. Weigh the clot on the weighing scale for assessing the clot mass loss.

8.5. To analyze the D-dimer content, add 100 mg of aminocaproic acid to a microcentrifuge tube followed by 1 mL of perfusate, and mix well using a pipette. Perform a latex immune-turbidimetric assay to quantify the D-dimer within the sample[36].

8.6. To assess hemolysis, add 1 mL of perfusate to centrifuge tubes and spin at 610 x *g* (3,500 rpm) for 10 min. Combine 0.5 mL of supernatant (concentrate) with 0.5 mL of Drabkins solution and let the mixture rest at room temperature for 15 min. Transfer 200 µL to well plates, as shown in **Figure 4B**. Use a plate reader to read absorbance at 540 nm, **Figure 4C** (Drabkins assay[37]).

8.7. Histology assessment

8.7.1. Cut a section from the center of the clot of about 2–3 mm in length with a scalpel.

8.7.2. Add the section to a cassette. Maintain orientation of the section relative to the direction of histotripsy pulse propagation.

8.7.3. Add 2 mL of low gelling agarose solution prepared in step 3.2.5 into the cassette to fix the clot in place.

8.7.4. Fix the sample in 10% formalin for 24 h. Place the sample in 70% alcohol after 24 h and perform standard hemotoxylin-eosin staining[38].

9. Passive cavitation image analysis

9.1. Process the signals acquired from the imaging array during the histotripsy excitation (step 7.2.4) using an algorithm based on the robust Capon beamformer[39] to create an image of bubble cloud activity at each treatment location.

NOTE: To generate quantitative images, follow the steps described in Haworth et al.[35]. Otherwise, each pixel value in the image should represent the relative bubble cloud acoustic energy (units of V^2) at each corresponding location.

9.2. Segment the B-mode image to distinguish between the pixels representing clot and the model vessel.

9.3. Average all the passive cavitation images obtained at each location temporally. Co-register the passive cavitation image with the B-mode image as shown in **Figure 5B**. Sum up the acoustic energy within the clot over the exposure period[35].

REPRESENTATIVE RESULTS:

The protocol outlined in this study highlights the details of venous clot modeling, lysotripsy for clot disruption, and ultrasound imaging in an in vitro setup of DVT. The adopted procedure demonstrates the steps necessary to assess clot disruption due to the combined effects of rt-PA and histotripsy bubble cloud activity. The benchtop setup was designed to mimic the characteristics of a venous iliofemoral vein. **Figure 1A** shows a model vessel that has the acoustic, mechanical, and geometrical properties of the iliofemoral vein. The clot is placed inside the model vessel to mimic a partially occlusive thrombus. The clot is perfused with plasma and rt-PA drawn from a reservoir at a rate of 0.65 mL/min. This rate is consistent with slow flow rate in a highly occluded vessel[34].

An elliptically focused transducer of 1.5 MHz fundamental frequency with a 9 cm major axis, 7 cm minor axis, and 6 cm focal length (**Figure 2A**) is mounted on the positioning system as noted in **Figure 1B**. An imaging array covered with ultrasound gel and a latex cover (**Figures 2B,C**) is mounted coaxially with the transducer as shown in **Figure 1A** via an opening in the center of the histotripsy source. The motorized positioners were used to translate the therapy

transducer/imaging array along the clot length within the model vessel (**Figure 1**). Upon application of sufficient voltage to the histotripsy source, a bubble cloud is generated in the focal region of the transducer and visualized via ultrasound imaging GUI, as shown in **Figure 3**. The focal position is defined as the center of the bubble cloud using the imaging GUI (steps 4.10–4.11).

Figure 4A shows perfusates collected for two different treatment conditions. The beaker labeled as control contains perfusate of a clot exposed to plasma alone. The second beaker labeled as treated contains the perfusate of the lysotripsy treated clot. The collected perfusates are used to assess the hemoglobin (metric of hemolysis) and D-dimer (metric of fibrinolysis) content through assays as specified in the protocol. The difference in color of the perfusates denotes variability in hemoglobin concentration, which can be quantified via optical absorbance. The relationship between absorbance value and hemoglobin concentration can be determined through a calibration curve. Solutions with known hemoglobin content ranging from 0 (blank measurement) to 180 mg/mL are placed in the well plate and absorbance is determined in triplicate using the plate reader (**Figure 4B,C).** The upper absorbance limit of the plate reader may vary and may not be known *a priori* to making the solutions in the well plate. As such, hemoglobin concentrations up to 180 mg/mL are made in the well plate, **Figure 4B**. However, the plate reader used here can read absorbance for concentrations up to 23 mg/mL only, **Figure 4C.**

Figure 5A shows visualization of the clot within the model vessel via B-mode imaging prior to histotripsy exposure as specified in step 7.2.3. This image is acquired to determine the clot position for segmentation of the passive cavitation image. **Figure 5B** shows the passive cavitation image co-registered with the B-mode image acquired prior to histotripsy exposure. This figure confirms that acoustic energy is contained primarily within the clot during histotripsy exposure.

Typical clot disruption due to histotripsy and lytic are indicated in **Figure 6**. **Figure 6A,B** show the untreated and lysotripsy treated clot images, respectively. For samples exposed to histotripsy, disruption is primarily restricted to the clot center, consistent with the observed locations of bubble activity tracked with passive cavitation imaging (**Figure 5B**). However, with addition of lytic, mass loss also occurs in regions closer to the periphery of the clot. It is hypothesized that this additional mass loss is due to enhanced fluid mixing of the lytic under bubble activity. Fluid mixing increases the distribution and penetration depth of the lytic into the clot. Since the lytic is responsible for fibrinolysis[40], the mass loss increases. Fibrinolysis can be quantified by measuring the D-dimer content in the perfusate[41].

FIGURE LEGENDS:

Figure 1: Experimental setup for lysotripsy of human blood clot. (**A**) The components of the setup are (1) focused histotripsy source with elliptical geometry, (2) latex-covered imaging array, (3) model vessel attached to flow channel, (4) flow channel, (5) reservoir, (6) acoustic absorbing material, (7) heating element, and (8) water tank filled with degassed and heated reverse osmosis water. The axial dimension of the imaging plane, not shown in the coordinate system, is

perpendicular to the elevational and range dimensions (into the page). (**B**) The histotripsy source mounted on the motorized positioning system.

Figure 2: Ultrasound source and imaging components. Individual zoomed images of (**A**) focused histotripsy source, (**B**) imaging array, and (**C**) imaging array with ultrasound gel and latex cover.

Figure 3: Histotripsy bubble cloud visualized using imaging array. A bubble cloud is generated in the focal zone of the histotripsy source and imaged using an imaging array. The designated focus, shown as a cross, is saved for treatment planning.

Figure 4: Quantification of hemoglobin released due to clot lysis. (**A**) Perfusate samples collected following control study with plasma alone (no histotripsy or lytic), and treatment arm, histotripsy (e.g., 35 MPa peak negative pressure, 5 cycle pulse duration, 1.5 MHz fundamental frequency), and 2.68 µg/mL lytic exposure. (**B**) Well plate containing dilutions of known hemoglobin concentrations ranging from 180 mg/mL (top row, left-most corner) to 0 mg/mL (bottom row, right-most corner). The arrowhead points toward decreasing hemoglobin concentration. (**C**) These samples are used to create a standard curve to quantify hemoglobin produced due to histotripsy exposure via spectrophotometry. Absorbance curve for hemoglobin concentrations ranging from 0 to 23 mg/mL is obtained due to limitation of the plate reader in analyzing higher concentrations.

Figure 5: Images of the clot during treatment. (**A**) B-mode image acquired before the start of treatment pulse showing the clot position within the model vessel. (**B**) Post-hoc visualization of acoustic energy emission calculated from passive cavitation imaging shown in hot colormap co-registered with B-mode image of the clot acquired prior to application of the histotripsy pulse.

Figure 6: Histology of the ablated clot under different treatment conditions. (**A**) Control clot without treatment. (**B**) Clot treated with histotripsy (e.g., 35 MPa peak negative pressure, single cycle pulse duration, 1.5 MHz fundamental frequency) and lytic. The histotripsy pulse propagated from top to bottom in this image. The path for the histotripsy source along the length of the clot (i.e., perpendicular to the plane of the image shown here) is defined in step 7.2.3. The scale of the micrographs is 2 mm. Note that the degree of clot disruption achieved here would be reduced compared to insonation schemes with longer pulse duration[24].

DISCUSSION:

The proposed protocol presents a model to quantify treatment efficacy of lysotripsy. While the key details have been discussed, there are certain critical aspects to consider for the success of this protocol. The enzymatic activity of rt-PA has an Arrhenius temperature dependence[30]. Temperature is also a contributing factor to the speed of sound in water and tissue, and variations in temperature can cause minor alterations of the focal zone geometry. Thus, the water temperature should be carefully regulated at 37 ˚C. The dose of rt-PA used in the protocol (2.68 µg/mL) is consistent with that employed clinically for other pharmacomechanical thrombectomy strategies[42]. In step 5.8, 30 mL of plasma is transferred to the reservoir whereas a 35 mL aliquot

is noted in step 3.1.3. This additional plasma accounts for loss in plasma due to evaporation over the course of hours when warmed to 37 ˚C for equilibration to atmospheric pressure.

The focal length, aperture width, and frequency of the therapy transducer dictate the size and depth of the focal region. Therefore, the transducer should be chosen such that these characteristics align with the diameter and the depth of the target vessel (e.g. femoral vein: 2–4 cm in depth and 0.6–1.2 cm in diameter)[43]. The extent of mechanical ablation is restricted to the extent of the bubble cloud. Thus, an understanding of the role insonation parameters play in modifying histotripsy bubble cloud behavior is critical[33,44,45]. The frequency and the strength of acoustic field should also be chosen noting the magnitude of attenuation due to medium and intermediary materials (e.g., model vessel). To ensure confinement of bubble activity with the target vessel, an appropriate imaging window should be chosen to monitor the focal zone. The operating parameters of the transducer should be chosen to avoid off target effects while maximizing mechanical clot disruption. In this protocol, mass loss was considered a primary metric of treatment efficacy. Increases in mass loss have been observed as the peak negative pressure or the duration of the histotripsy pulse are increased[24,46], with a maximum observed mass loss of 94%. The presence of residual clot for investigated treatment arms facilitates comparison of therapeutic efficacy. However, insonation schemes to ensure total removal of the thrombus can also be devised.

The acoustic impedance (approximately 1.58 MRayl[47,48]) and the geometrical properties (0.6–1.2 cm in diameter[43]) of the model vessel should be representative of the iliofemoral venous vasculature (see **Table of Materials** for details). Polydimethylsiloxane and polyurethane are some of the materials suitable to model the venous system based on their acousto-mechanical properties. In step 7, it is important to remove all the air bubbles from the model vessel to avoid shielding the clot from histotripsy exposure. For a model vessel of hydrophobic material, bubble clouds may form preferentially near the vessel wall instead of the center of the clot. Therefore, continuous monitoring of the bubble cloud should be done during the treatment via ultrasound imaging, and the transducer should be repositioned, if necessary. Pilot studies should be conducted to determine histotripsy insonation parameters (e.g., pulse duration and peak pressure) that achieve the final intended clot disruption.

The imaging array is used to capture B-mode images and passive cavitation images for treatment visualization and to quantify bubble activity. B-mode imaging allows visualization of the model vessel and the clot, and passive cavitation imaging gauges the energy of the bubble activity associated with clot ablation[24,49]. The bandwidth of the imaging array should align with the desired bubble cloud activity with a high signal-to-noise ratio. For purely broadband signals associated with the inertial collapse of bubbles within the cloud, the bandwidth of the array should not coincide with the fundamental frequency of the transducer[50,51]. Histotripsy pulses are highly nonlinear[52], and it is likely that harmonics of the fundamental frequency will be present in the received signal. The imaging system should be programmed to trigger on based on the known time of flight of the histotripsy pulse from the source to the focal zone, to ensure collection of passive cavitation imaging data throughout the insonation. These signals should then be processed post hoc as discussed in steps 7.2.3 and 9 of the protocol.

It should be noted that the amount of hemolysis is sensitive to the handling of the clot. Therefore, care should be taken to minimize damage to the clot before treatment. To ensure reproducibility, clot modelling (step 1) and pre-treatment time (steps 6 and 7.1) should be same for all the clots treated with or without histotripsy exposure. In the post-treatment step of hemolysis assessment, it should be noted that plasma has its own absorbance. Therefore, the diluent used to form standard curves (e.g., optical absorbance vs. hemoglobin) should be formed using the same fluid used as the perfusate in the flow channel (e.g., in this study, plasma was used as the diluent to form standard curves).

This protocol aims to provide a benchtop setup to gauge the efficacy of lysotripsy to treat human whole blood clots. There are certain limitations that arise due to the in vitro nature of the set up. The acute clots used for this protocol composed mainly of red blood cells and fibrin, making the approach of lysotripsy effective for DVT. However, later stages of thrombus may develop a stiff collagenous network[53] that may resist the lysotripsy treatment due to the fibrin-specific nature of rt-PA. When treating in vivo, the primary clinical endpoint for treatment efficacy is restoration of flow. Mass loss was a primary metric for treatment efficacy in the in vitro protocol described here. Although flow was not assessed in this protocol, color Doppler imaging can be additionally incorporated along with passive cavitation imaging in step 7.2.4 to monitor flow restoration. The setup in this protocol uses a fixed flow rate, mimicking the flow rate in a highly occluded vessel, during the entire treatment in step 7.2. In vivo, vascular flow will increase as the clot disintegrates during the treatment. The additional shear stresses associated with increased flow will accentuate the clot degradation profile[54]. In vivo off-target effects cannot be ascertained in this setup, such as bleeding due to systemic administration of lytic[55], vessel wall damage or vasospasm due to bubble cloud activity[22]. The in vitro nature of this study also limits the ability to assess long-term outcomes, such as vessel patency or re-thrombosis after treatment. The administration of lytic in this study mimicked systemic thrombolytics, whereas catheter-directed lytics is the preferred intervention for venous thrombosis[7,14]. Tissue attenuation can affect the histotripsy field and the imaging quality for in vivo studies, whereas here the acoustic path is primarily through degassed water. Processing of cavitation emission data with the robust Capon beamformer (step 9 of the protocol) is computationally expensive and was conducted off-line for *post hoc* analysis. Other beamformers (e.g., delay-and-sum[35] or angular spectrum[56]) can be operated alternatively to provide real-time feedback, albeit with reduced range resolution.

In summary, this protocol presents a non-invasive approach to achieve deep vein thrombolysis of human blood clots. The protocol establishes a convenient and easy-to-replicate procedure for modeling of blood clots, treating them with lysotripsy, and simultaneous imaging during treatment. The protocols specifying histotripsy bubble cloud generation, treatment planning, and image guidance can be further used to investigate in vitro treatments of breast tumor, pancreatic tumor, and benign prostatic hyperplasia, where histotripsy has been shown to be more effective as compared to standard procedures[57,58]. The use of rt-PA in this protocol can be generalized to other drugs or drug carriers that are used for treating such tumors, along with histotripsy to increase the lytic efficacy.

ACKNOWLEDGMENTS:

This work was funded by the National Institutes of Health, Grant R01HL13334. The authors would like to thank Dr. Kevin Haworth for assisting with Drabkin's assay and Dr. Viktor Bollen for his support in designing the protocol. The authors are also thankful to Dr. Adam Maxwell for his guidance on designing the histotripsy source.

DISCLOSURES:

The authors have nothing to disclose.

REFERENCES:

1. Oklu, R. Thrombosis. *Cardiovascular Diagnosis and Therapy*. **7** (Suppl 3), S131–S133 (2017).
2. Satoh, K., Satoh, T., Yaoita, N., Shimokawa, H. Recent advances in the understanding of thrombosis. *Arteriosclerosis, Thrombosis, and Vascular Biology*. **39** (6), e159–e165 (2019).
3. Grosse, S. D., Nelson, R. E., Nyarko, K. A., Richardson, L. C., Raskob, G. E. The economic burden of incident venous thromboembolism in the United States: A review of estimated attributable healthcare costs. *Thrombosis Research*. **137**, 3–10 (2016).
4. Hirsh, J., Hoak, J. Management of deep vein thrombosis and pulmonary embolism. *Circulation*. **93** (12), 2212–2245 (1996).
5. Browse, N. L., Clemenson, G., Croft, D. N. Fibrinogen-detectable thrombosis in the legs and pulmonary embolism. *British Medical Journal*. **1** (5908), 603–604 (1974).
6. Plate, G., Ohlin, P., Eklöf, B. Pulmonary embolism in acute iliofemoral venous thrombosis. *British Journal of Surgery*. **72** (11), 912–915 (1985).
7. Chen, J. X., Sudheendra, D., Stavropoulos, S. W., Nadolski, G. J. Role of catheter-directed thrombolysis in management of iliofemoral deep venous thrombosis. *Radiographics*. **36** (5), 1565–1575 (2016).
8. Kahn, S. R., Solymoss, S., Lamping, D. L., Abenhaim, L. Long-term outcomes after deep vein thrombosis: postphlebitic syndrome and quality of life. *Journal of General Internal Medicine*. **15** (6), 425–429 (2000).
9. Oğuzkurt, L., Ozkan, U., Gülcan, O., Koca, N., Gür, S. Endovascular treatment of acute and subacute iliofemoral deep venous thrombosis by using manual aspiration thrombectomy: long-term results of 139 patients in a single center. *Diagnostic and Interventional Radiology*. **18** (4), 410–416 (2012).
10. Lauw, M. N., Büller, H. R. in *Current Approaches to Deep Vein Thrombosis*. 136–160 (2014).
11. Kearon, C. et al. Antithrombotic therapy for VTE disease: antithrombotic therapy and prevention of thrombosis: American college of chest physicians evidence-based clinical practice guidelines. *Chest*. **141** (2), e419S–e496S (2012).
12. Pouncey, A. L. et al. AngioJet Pharmacomechanical Thrombectomy and Catheter Directed Thrombolysis vs. Catheter Directed Thrombolysis Alone for the Treatment of Iliofemoral Deep Vein Thrombosis: A Single Centre Retrospective Cohort Study. *European Journal of Vascular and Endovascular Surgery*. (2020).
13. Tang, T., Chen, L., Chen, J., Mei, T., Lu, Y. Pharmacomechanical thrombectomy versus catheter-directed thrombolysis for iliofemoral deep vein thrombosis: a meta-analysis of clinical trials. *Clinical and Applied Thrombosis/Hemostasis*. **25** (2019).

14. Kuo, T.-T., Huang, C.-Y., Hsu, C.-P., Lee, C.-Y. Catheter-directed thrombolysis and pharmacomechanical thrombectomy improve midterm outcome in acute iliofemoral deep vein thrombosis. *Journal of the Chinese Medical Association*. **80** (2), 72–79 (2017).
15. Donaldson, C. W. et al. Thrombectomy using suction filtration and veno-venous bypass: single center experience with a novel device. *Catheterization and Cardiovascular Interventions*. **86** (2), E81–87 (2015).
16. Khokhlova, V. A. et al. Histotripsy methods in mechanical disintegration of tissue: Towards clinical applications. *International Journal of Hyperthermia*. **31** (2), 145–162 (2015).
17. Bader, K. B., Vlaisavljevich, E., Maxwell, A. D. For whom the bubble grows: Physical principles of bubble nucleation and dynamics in histotripsy ultrasound therapy. *Ultrasound in Medicine & Biology*. **45** (5), 1056–1080 (2019).
18. Maxwell, A. D. et al. Noninvasive thrombolysis using pulsed ultrasound cavitation therapy–histotripsy. *Ultrasound in Medicine & Biology*. **35** (12), 1982–1994 (2009).
19. Xu, Z. et al. Size measurement of tissue debris particles generated from pulsed ultrasound cavitational therapy-histotripsy. *Ultrasound in Medicine & Biology*. **35** (2), 245–255 (2009).
20. Vlaisavljevich, E. et al. Effects of tissue stiffness, ultrasound frequency, and pressure on histotripsy-induced cavitation bubble behavior. *Physics in Medicine and Biology*. **60** (6), 2271–2292 (2015).
21. Zhang, X. et al. Histotripsy thrombolysis on retracted clots. *Ultrasound in Medicine & Biology*. **42** (8), 1903–1918 (2016).
22. Maxwell, A. D. et al. Noninvasive treatment of deep venous thrombosis using pulsed ultrasound cavitation therapy (histotripsy) in a porcine model. *Journal of Vascular and Interventional Radiology*. **22** (3), 369–377 (2011).
23. Bader, K. B. et al. Efficacy of histotripsy combined with rt-PA in vitro. *Physics in Medicine and Biology*. **61** (14), 5253–5274 (2016).
24. Bollen, V. et al. In vitro thrombolytic efficacy of single- and five-cycle histotripsy pulses and rt-PA. *Ultrasound in Medicine & Biology*. **46** (2), 336–349 (2020).
25. Wang, Y. N., Khokhlova, T., Bailey, M., Hwang, J. H., Khokhlova, V. Histological and biochemical analysis of mechanical and thermal bioeffects in boiling histotripsy lesions induced by high intensity focused ultrasound. *Ultrasound in Medicine & Biology*. **39** (3), 424–438 (2013).
26. Weisel, J. W., Litvinov, R. I. Fibrin formation, structure and properties. *Sub-Cellular Biochemistry*. **82**, 405–456 (2017).
27. Devanagondi, R. et al. Hemodynamic and hematologic effects of histotripsy of free-flowing blood: implications for ultrasound-mediated thrombolysis. *Journal of Vascular and Interventional Radiology: JVIR*. **26** (10), 1559–1565 (2015).
28. Holland, C. K., Vaidya, S. S., Datta, S., Coussios, C.-C., Shaw, G. J. Ultrasound-enhanced tissue plasminogen activator thrombolysis in an in vitro porcine clot model. *Thrombosis Research*. **121** (5), 663–673 (2008).
29. Sutton, J. T., Ivancevich, N. M., Perrin, S. R., Jr., Vela, D. C., Holland, C. K. Clot retraction affects the extent of ultrasound-enhanced thrombolysis in an ex vivo porcine thrombosis model. *Ultrasound in Medicine & Biology*. **39** (5), 813–824 (2013).
30. Shaw, G. J., Dhamija, A., Bavani, N., Wagner, K. R., Holland, C. K. Arrhenius temperature dependence of in vitro tissue plasminogen activator thrombolysis. *Physics in Medicine & Biology*. **52** (11), 2953 (2007).

31. Pinto, J. et al. Human plasma stability during handling and storage: impact on NMR metabolomics. *Analyst*. **139** (5), 1168–1177 (2014).
32. Shaw, G. J., Sperling, M., Meunier, J. M. Long-term stability of recombinant tissue plasminogen activator at -80 C. *BMC Research Notes*. **2** (1), 117 (2009).
33. Maxwell, A. D. et al. Cavitation clouds created by shock scattering from bubbles during histotripsy. *The Journal of the Acoustical Society of America*. **130** (4), 1888–1898 (2011).
34. Jensen, C. T. et al. Qualitative slow blood flow in lower extremity deep veins on doppler sonography: quantitative assessment and preliminary evaluation of correlation with subsequent deep venous thrombosis development in a tertiary care oncology center. *Journal of Ultrasound in Medicine*. **36** (9), 1867–1874 (2017).
35. Haworth, K. J., Bader, K. B., Rich, K. T., Holland, C. K., Mast, T. D. Quantitative frequency-domain passive cavitation imaging. *IEEE Transactions on Ultrasonics, Ferroelectrics, and Frequency Control*. **64** (1), 177–191 (2017).
36. Hamano, A. et al. Latex immunoturbidimetric assay for soluble fibrin complex. *Clinical Chemistry*. **51** (1), 183–188 (2005).
37. Drabkin, D. L., Austin, J. H. Spectrophotometric studies II. Preparations from washed blood cells; nitric oxide hemoglobin and sulfhemoglobin. *Journal of Biological Chemistry*. **112** (1), 51–65 (1935).
38. Fischer, A. H., Jacobson, K. A., Rose, J., Zeller, R. Hematoxylin and eosin staining of tissue and cell sections. *CSH Protocols*. **2008** (2008).
39. Coviello, C. et al. Passive acoustic mapping utilizing optimal beamforming in ultrasound therapy monitoring. *The Journal of the Acoustical Society of America*. **137** (5), 2573–2585 (2015).
40. Mori, K., Dwek, R. A., Downing, A. K., Opdenakker, G., Rudd, P. M. The activation of type 1 and type 2 plasminogen by type I and type II tissue plasminogen activator. *Journal of Biological Chemistry*. **270** (7), 3261–3267 (1995).
41. Righini, M., Perrier, A., De Moerloose, P., Bounameaux, H. D-Dimer for venous thromboembolism diagnosis: 20 years later. *Journal of Thrombosis and Haemostasis: JTH*. **6** (7), 1059–1071 (2008).
42. Hilleman, D. E., Razavi, M. K. Clinical and economic evaluation of the Trellis-8 infusion catheter for deep vein thrombosis. *Journal of Vascular and Interventional Radiology: JVIR*. **19** (3), 377–383 (2008).
43. De Sensi, F. et al. Predictors of successful ultrasound guided femoral vein cannulation in electrophysiological procedures. *Journal of Atrial Fibrillation*. **11** (3), 2083–2083 (2018).
44. Vlaisavljevich, E. et al. Effects of ultrasound frequency and tissue stiffness on the histotripsy intrinsic threshold for cavitation. *Ultrasound in Medicine & Biology*. **41** (6), 1651–1667 (2015).
45. Vlaisavljevich, E. et al. Histotripsy-induced cavitation cloud initiation thresholds in tissues of different mechanical properties. *IEEE Transactions on Ultrasonics, Ferroelectrics, and Frequency Control*. **61** (2), 341–352 (2014).
46. Hendley, S. A., Paul, J. D., Bader, K. B. Mechanistic investigation of clot degradation via the action of histotripsy and thrombolytic. *Joint AAPM | COMP Virtual Meeting. The American Association of Physics in Medicine.* (2020).

47. Goss, S. A., Johnston, R. L., Dunn, F. Comprehensive compilation of empirical ultrasonic properties of mammalian tissues. *The Journal of the Acoustical Society of America*. **64** (2), 423–457 (1978).
48. Duck, F. A. in *Physical Properties of Tissues* (Ed Francis A. Duck). Academic Press. 137–165 (1990).
49. Bader, K. B., Haworth, K. J., Maxwell, A. D., Holland, C. K. Post hoc analysis of passive cavitation imaging for classification of histotripsy-induced liquefaction in vitro. *IEEE Transactions on Medical Imaging*. **37** (1), 106–115 (2018).
50. Crake, C. et al. Enhancement and passive acoustic mapping of cavitation from fluorescently tagged magnetic resonance-visible magnetic microbubbles in vivo. *Ultrasound in Medicine & Biology*. **42** (12), 3022–3036 (2016).
51. Gyongy, M., Coussios, C. Passive spatial mapping of inertial cavitation during HIFU exposure. *IEEE Transactions on Biomedical Engineering*. **57** (1), 48–56 (2010).
52. Canney, M. S., Bailey, M. R., Crum, L. A., Khokhlova, V. A., Sapozhnikov, O. A. Acoustic characterization of high intensity focused ultrasound fields: A combined measurement and modeling approach. *The Journal of the Acoustical Society of America*. **124** (4), 2406–2420 (2008).
53. Czaplicki, C. et al. Can thrombus age guide thrombolytic therapy? *Cardiovascular Diagnosis and Therapy*. **7** (Suppl 3), S186–S196 (2017).
54. Bajd, F., Vidmar, J., Blinc, A., Sersa, I. Microscopic clot fragment evidence of biochemo-mechanical degradation effects in thrombolysis. *Thrombosis Research*. **126** (2), 137–143 (2010).
55. Wang, C. et al. Efficacy and safety of low dose recombinant tissue-type plasminogen activator for the treatment of acute pulmonary thromboembolism: a randomized, multicenter, controlled trial. *Chest*. **137** (2), 254–262 (2010).
56. Arvanitis, C. D., Crake, C., McDannold, N., Clement, G. T. Passive acoustic mapping with the angular spectrum method. *IEEE Transactions on Medical Imaging.* **36** (4), 983–993 (2017).
57. Khokhlova, V. A. et al. Histotripsy methods in mechanical disintegration of tissue: towards clinical applications. *International Journal of Hyperthermia: The Official Journal of European Society for Hyperthermic Oncology, North American Hyperthermia Group*. **31** (2), 145–162 (2015).
58. Roberts, W. W. Development and translation of histotripsy: current status and future directions. *Current Opinion in Urology*. **24** (1), 104–110 (2014).

Figure 1

(A)

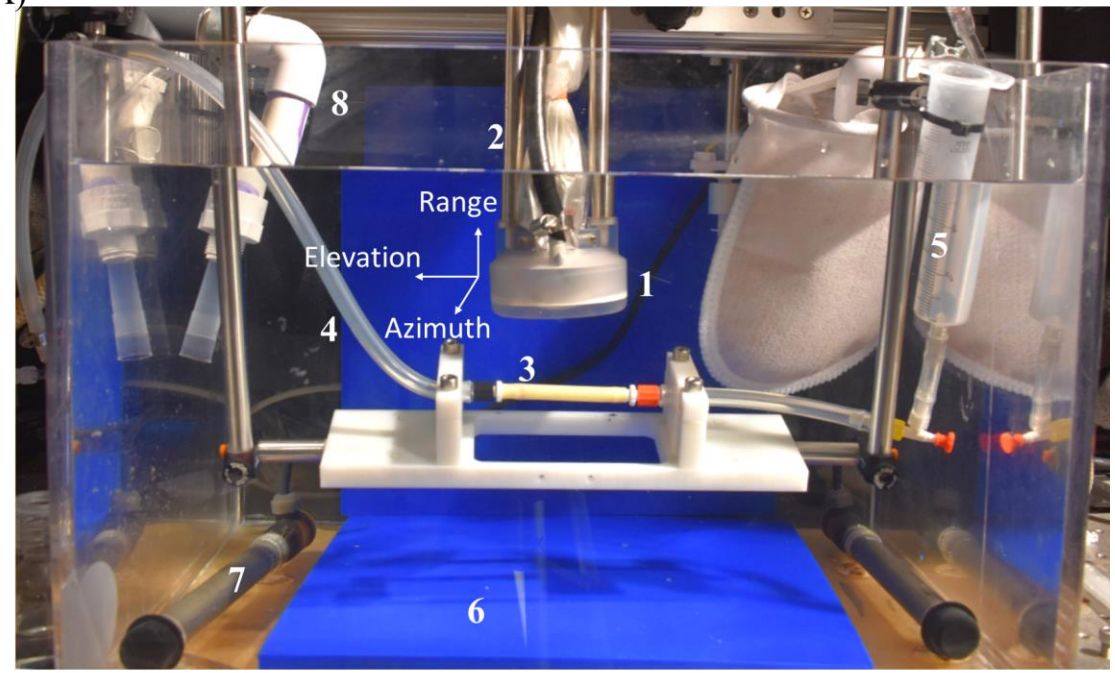

(B)

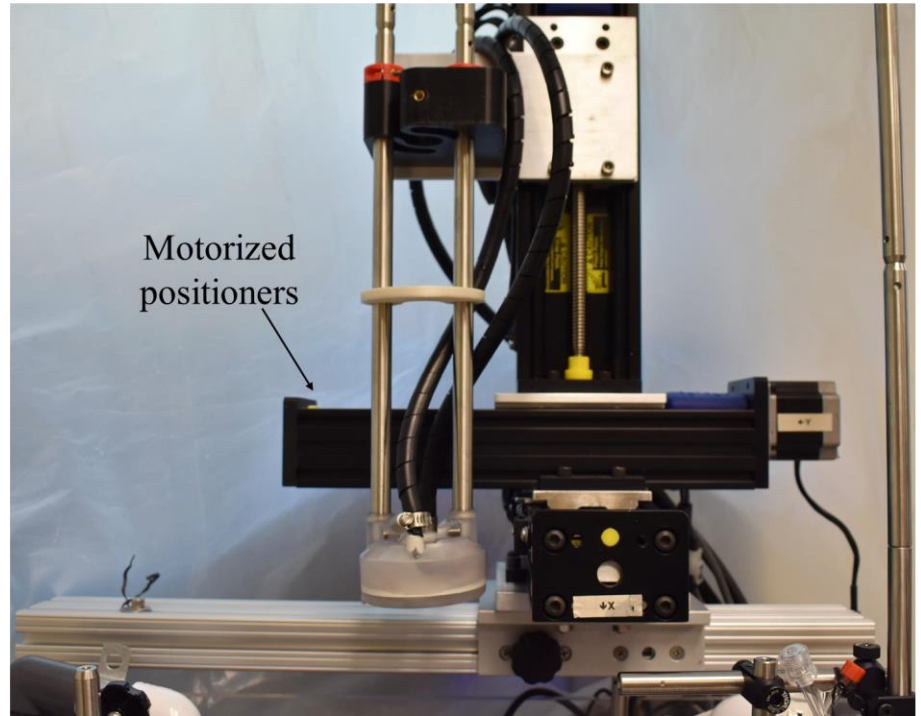

Figure 2

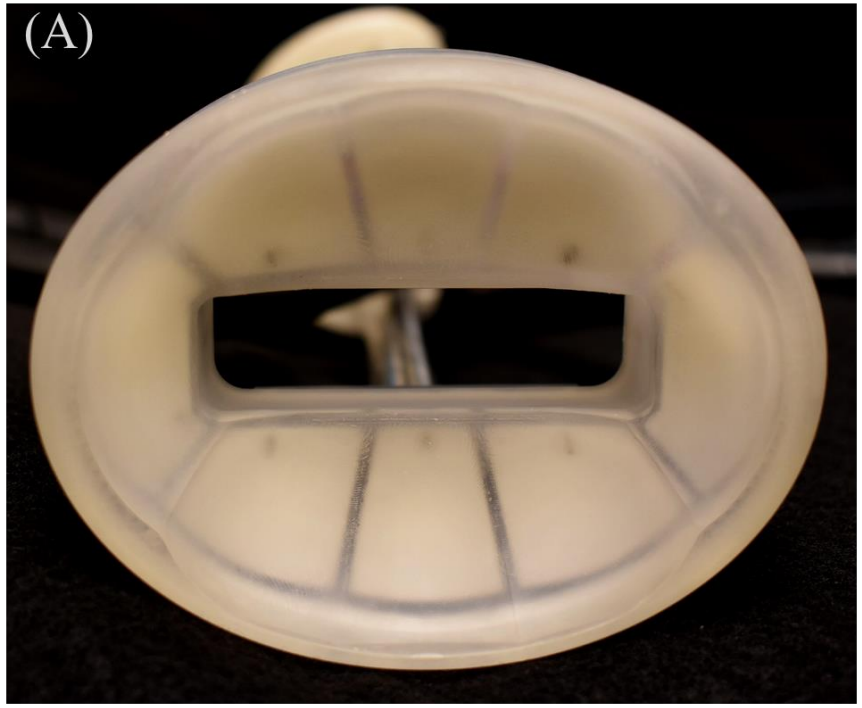

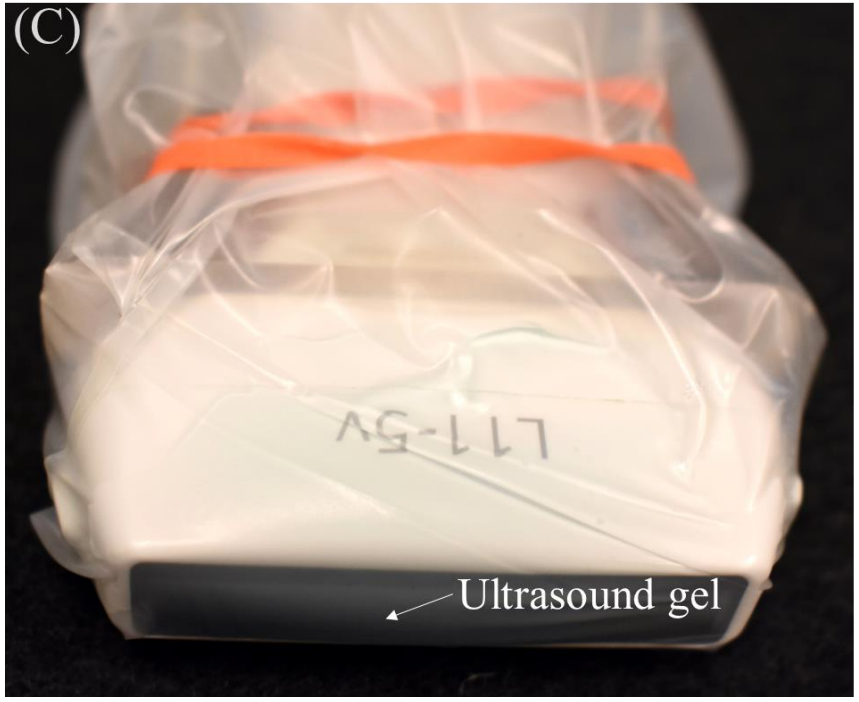

Figure 3

Click here to access/download;Figure;Figure 3.pdf

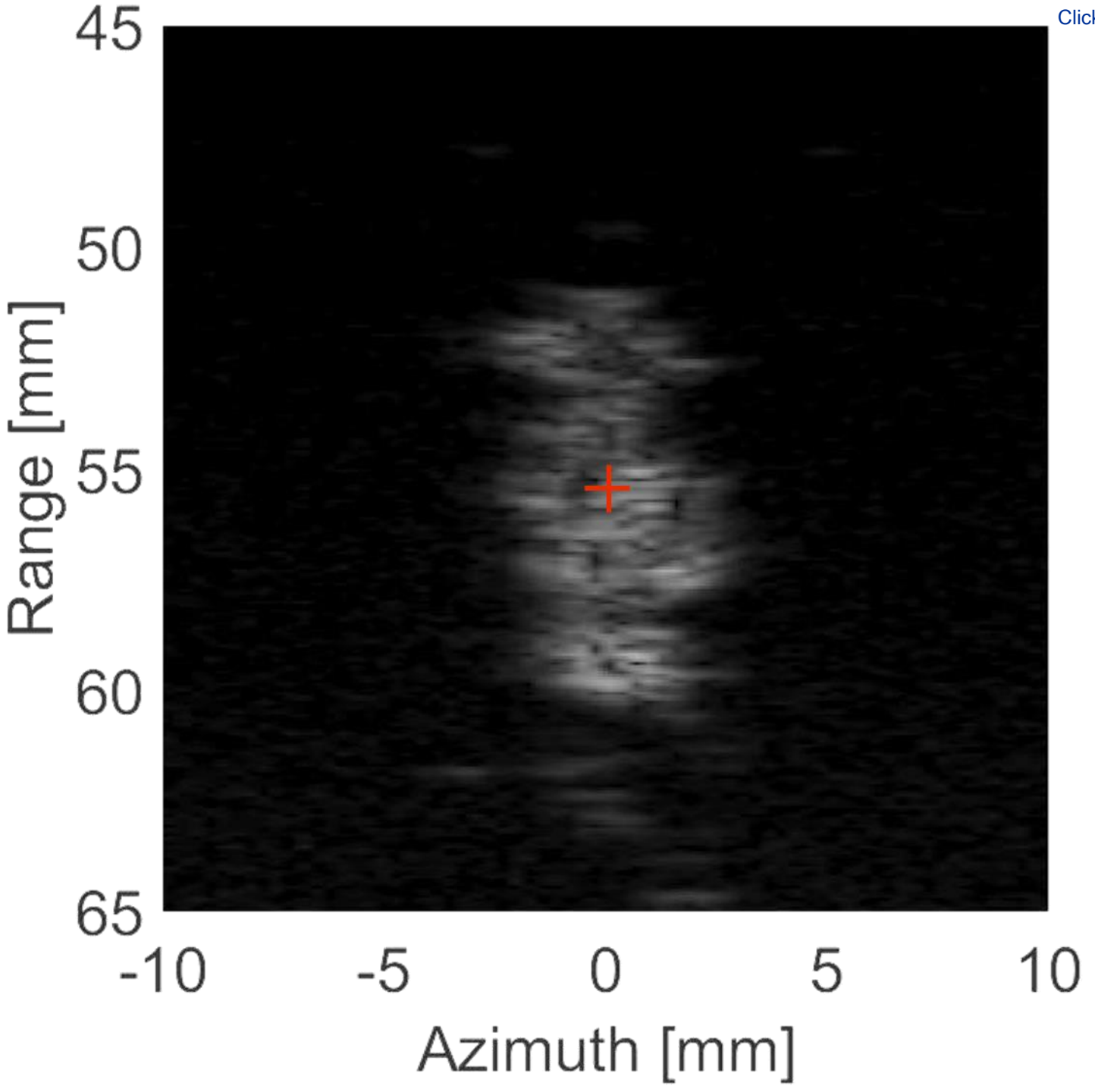

Figure 4

(A)

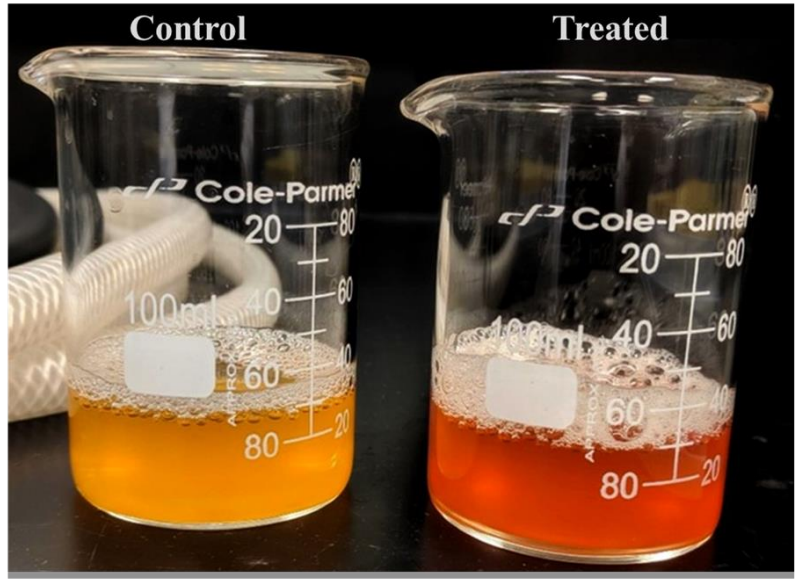

(B)

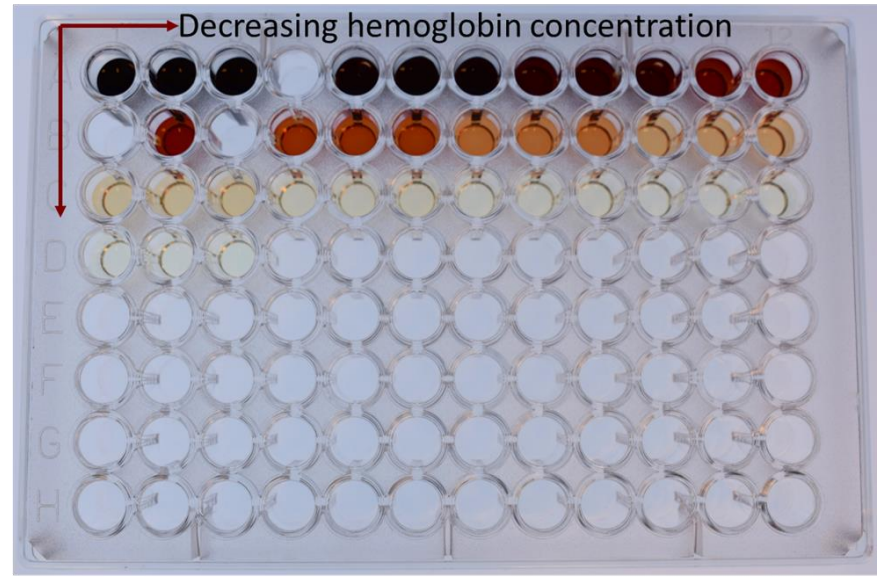

(C)

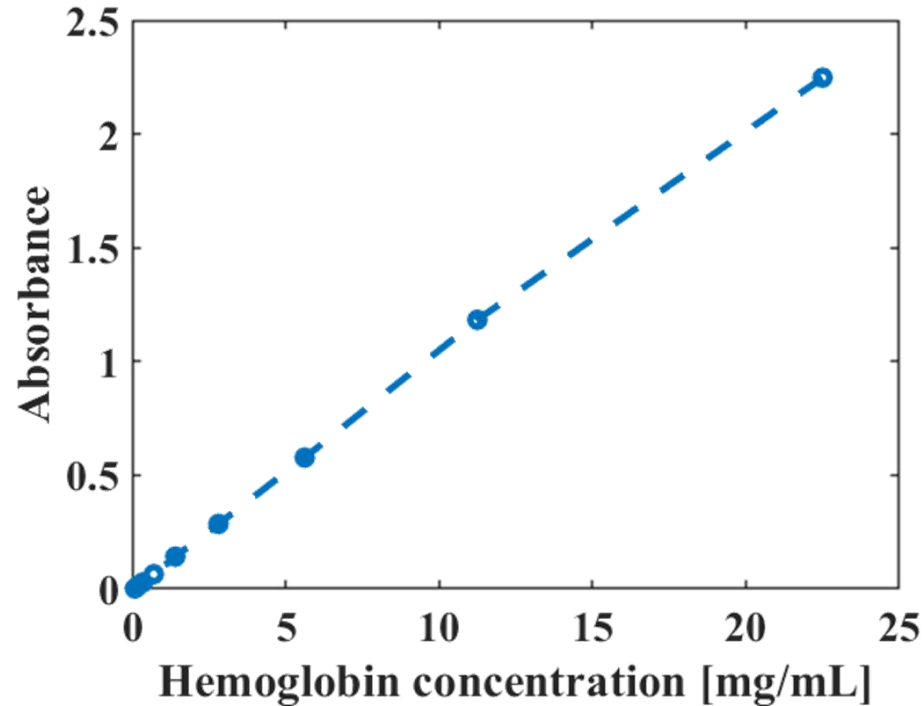

Figure 5

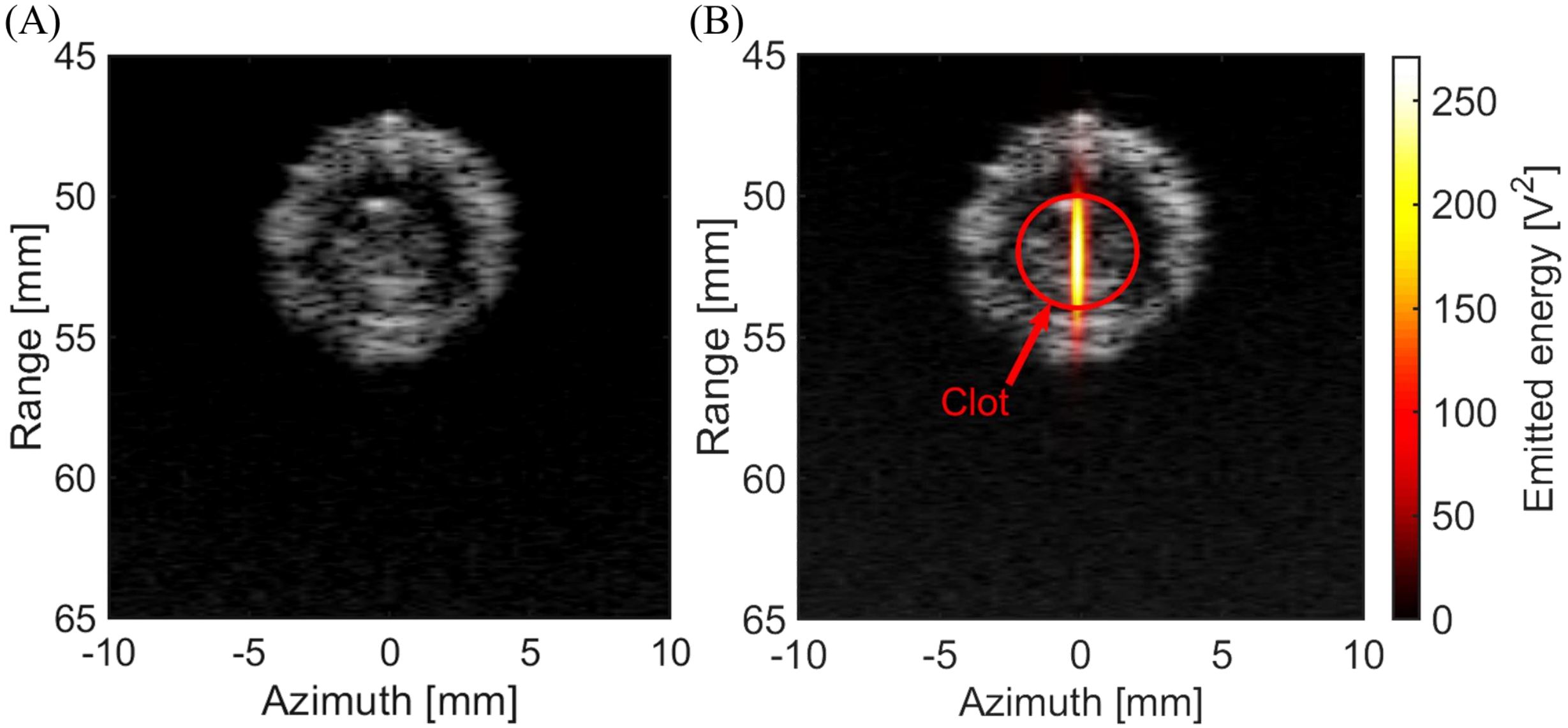

Figure 6

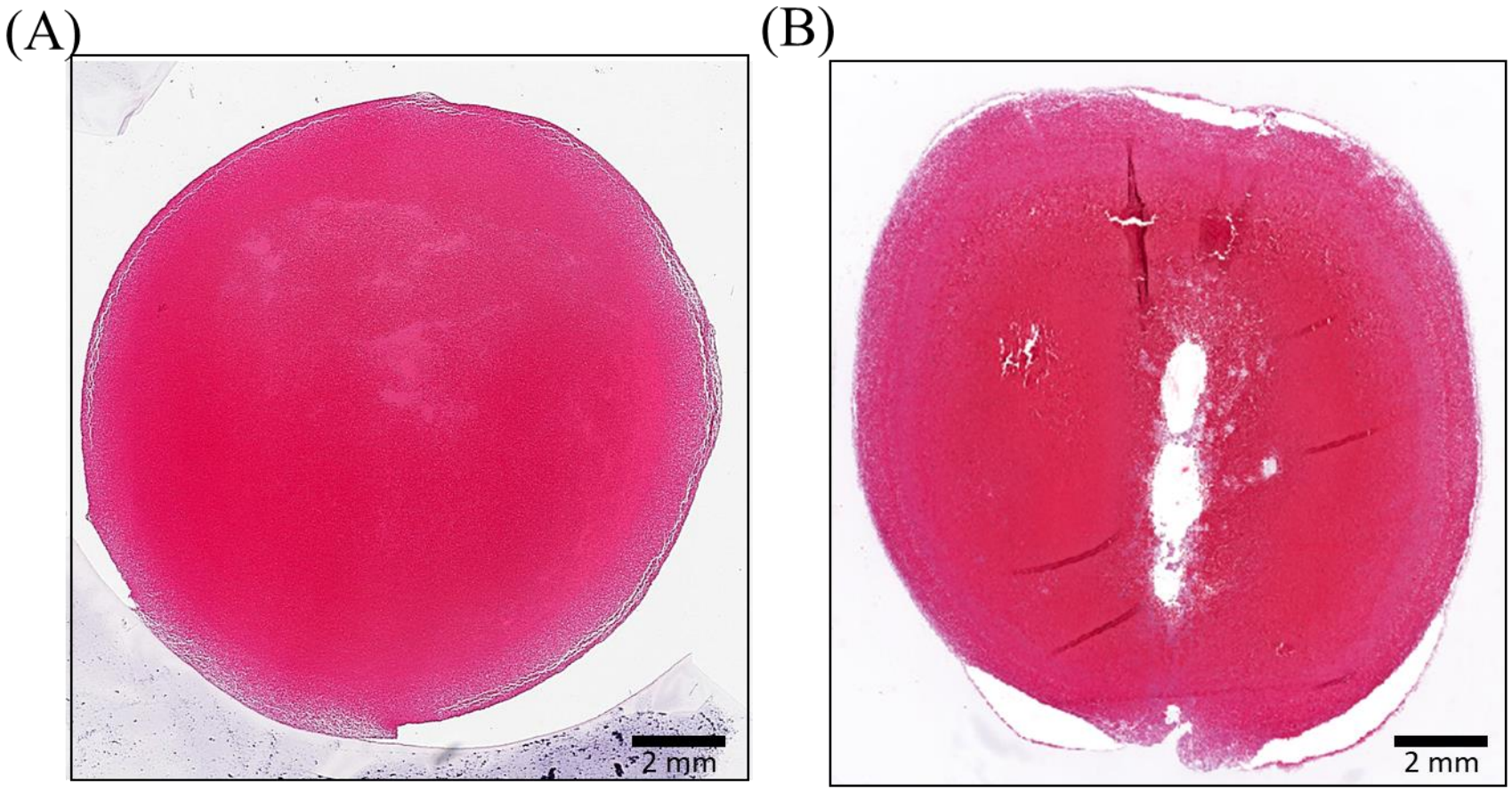

Table of Materials

Name of Material/ Equipment	Company	Catalog Number
Absorbing sheets	Precision acoustics	F28-SMALL-M
Borosilicate Pasteur pippettes	Fisher Scientific	1367820A
Centrifuge tubes	Eppendorf	22364111
Drabkin's assay	Sigma Aldrich	D5941-6VL
Draw syringe	Cole-Parmer	EW-07945-43
Filter bags	McMaster-Carr	5162K111
Flow channel tubing	McMaster-Carr	5154K25
Heating elements	Won Brothers	HT 300 Titanium
Imaging array	Verasonics	L11-5v
Low gelling agarose	Millipore Sigma	A9414
Model vessel	McMaster-Carr	5234K98
Nanopure water	Barnstead	Nanopure Diamond
Plasma	Vitalant	4PF000
Plate reader	Biotek	Synergy Neo HST Plate Reade
Probe cover	Civco	610-362
Programming platform	MATLAB (the Mathworks, Natick, MA, USA)	
Recombinant tissue-type plasminogen activator (rt-PA)	Genentech	Activase
Reservoir	Cole-Parmer	EW-07945-43
Syringe pump	Cole-Parmer	EW-74900-20
Transducer	In-house customized	

Ultrasound scaning system	Verasonics	
Water tank	Advanced acrylics	C133

Comments/Description
300mm x 300 mm x 10 mm
14.6 cm length, 2 mL capacity
1.5 mL capacity
60 mL capacity Remove particle size upto 1 microns Polyethylene-lined EVA plastic tubing (Outer diameter: 3/8", Inner diameter: 1/4" Titanium rods placed at the bottom of tank 128 element with sensitivity from -55 to -49 dB
6.6 cm length, 0.6 cm inner diameter, 1 mm thickness ASTM type I, 18 Mohm-cm resistivity Plasma frozen within 24 hours For haemoglobin quantification
60 mL capacity pump attached to the syringe to draw the flow in the flow channel at a pre-determined fized rate Eight-element, elliptically-focused transducer (9 cm major axis, 7 cm minor axis and 6 cm focal length), powered by custom designed and built class D amplifier and matching network

Vantage Research Ultrasound System
14 x 14 x 12, 1/2"

November 19, 2020

Dear Editor, Associate Editor, and Editorial Staff:

We are grateful to the reviewers for their valuable comments that led to a significant improvement of the original manuscript. Their comments (given in *italic* below) which have been addressed below and in the revised manuscript (seen as track changes in the manuscript and highlighted in blue here).

Sincerely yours,

Aarushi Bhargava, Ph.D.
Corresponding author

Manuscript # JoVE62133

Editorial comments (Comments to the Author):

We thank the editor for the helpful comments. Below are the corrections made for each of the comments:

1. *Please take this opportunity to thoroughly proofread the manuscript to ensure that there are no spelling or grammar issues. Please define all abbreviations at first use.*

   The text has been revised and any issues related to grammar, abbreviations, and the spelling have been resolved.

2. *JoVE cannot publish manuscripts containing commercial language. This includes trademark symbols (™), registered symbols (®), and company names before an instrument or reagent. Please remove all commercial language from your manuscript and use generic terms instead. All commercial products should be sufficiently referenced in the Table of Materials and Reagents.*

   For example: MATLAB (the Mathworks, Natick, MA, USA); Kimwipe; Vantage Research Ultrasound System (Verasonics, Inc., Kirkland, WA, USA) etc

   The text has been revised and the company names have been replaced with generic descriptions.

3. *To specify that this study had approval, please include an ethics statement before the numbered protocol steps, indicating that the protocol follows the guidelines of your institution's human research ethics committee*

The human blood clot preparation in this study was done according to University of Chicago review board protocol. The same has been added in step 1 of the manuscript (line 92 of page 3) as follows

For the results presented here, venous human blood was drawn to form clots after local internal review board approval (IRB #139-1300) and written informed consent provided to volunteer donors[1]

4. *Please ensure that all text in the protocol section is written in the imperative tense as if telling someone how to do the technique (e.g., "Do this," "Ensure that," etc.). The actions should be described in the imperative tense in complete sentences wherever possible. Avoid usage of phrases such as "could be," "should be," and "would be" throughout the Protocol. Any text that cannot be written in the imperative tense may be added as a "Note." However, notes should be concise and used sparingly. Please include all safety procedures and use of hoods, etc*

   The protocol has been revised to be written in the imperative tense.

5. *Please note that your protocol will be used to generate the script for the video and must contain everything that you would like shown in the video. Please add more details to your protocol steps. Please ensure you answer the "how" question, i.e., how is the step performed? Alternatively, add references to published material specifying how to perform the protocol action. Please add more specific details (e.g., button clicks for software actions, numerical values for settings, etc) to your protocol steps. There should be enough detail in each step to supplement the actions seen in the video so that viewers can easily replicate the protocol*

   The protocol has been revised to include more details about how the step is performed. We have also modified the protocol to quantify the range of parameter settings used to generate the histotripsy excitation and provide image guidance.

6. *1.2 and1.3: How many 2 mL aliquots are to be drawn and incubated?*

A 2 mL aliquot is used to form a single blood clot. Therefore, the total amount of blood drawn depends on the total number of clots that will be formed. The corrections in the manuscript for steps 1.1 and 1.2 (lines 99 – 104 of page 3) are as follows

1.2. Draw fresh human venous blood. Aliquot the total blood drawn in 2 mL increments per desired clot. Transfer each 2 mL aliquot to one Pasteur pipette.

NOTE: Execute step 1.2 within approximately 3 minutes so that blood does not clot before transferring to pipettes.

1.3. Incubate the blood aliquots within the pipettes (equal to the number of clots required) in a water bath for 3 hours at 37 °C.

7. *3.2.5: How much low gelling agarose (2%) is to be taken?*

Approximately 2 mL of agarose is needed for each sectioned sample. The total amount of agarose therefore will depend on the number of samples to be analyzed. The correction in step 3.2.5 of the manuscript (line 147 of page 5) is as follows

3.2.5. Make low gelling agarose (2%) in a 50 mL flask, by dissolving agarose in nanopure water. Choose the total amount of agarose solution such that approximately 2 mL is available for each specimen to be analyzed. Heat the solution in a microwave until bubbly. Secure the flask with a waterproof screw lid on it. Submerge the flask in the water bath alongside the plasma. This step ensures agarose is available to secure exposed clot segments for histology analysis following histotripsy insonation.

8. *Please highlight up to 3 pages of the Protocol (including headings and spacing) that identifies the essential steps of the protocol for the video, i.e., the steps that should be visualized to tell the most cohesive story of the Protocol. Remember that non-highlighted Protocol steps will remain in the manuscript, and therefore will still be available to the reader*

   The essential steps in the protocol to be included in the video, have been highlighted.

9. *Please include a scale bar for all images taken with a microscope to provide context to the magnification used. Define the scale in Figure 6's Legend.*

   The scale bar has been included in Figure 6 and the corresponding legend (line 415 of page 12) has been revised. The correction is as follows

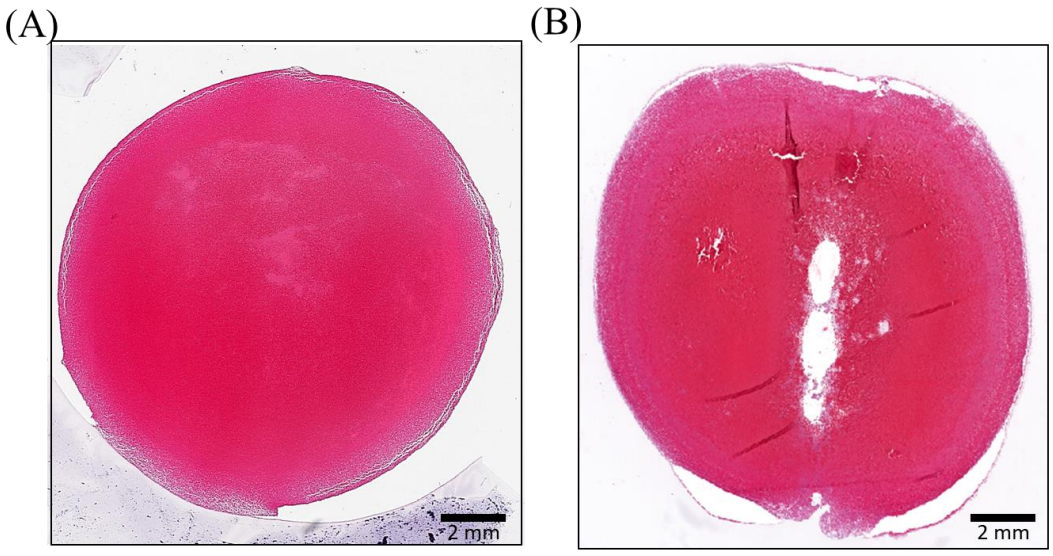

Figure 6. Histology of the ablated clot under different treatment conditions. **(A)** Control clot without treatment. **(B)** Clot treated with histotripsy (e.g. 35 MPa peak negative pressure, single cycle pulse duration, 1.5 MHz fundamental frequency) and lytic. The histotripsy pulse propagated from top to bottom in this image. The path for the histotripsy source along the length of the clot (i.e. perpendicular to the plane of the image shown here) is defined in step 7.2.3. The scale of the micrographs is 2 mm. Note that the degree of clot disruption achieved here would be reduced compared to insonation schemes with longer pulse duration[1].

Reviewer #1 (Comments to the Author):

Manuscript Summary:

This paper provides a detailed protocol to evaluate the thrombolytic efficacy in vitro using histotripsy combined with rt-PA. Histotripsy is a non-invasive ultrasound technique that mechanically breaks up the target tissue via cavitation. Histotripsy has been investigated to remove blood clots for treatment of thrombosis. The authors' work on histotripsy combined with rt-PA to enhance the thrombolytic efficacy is new. Their setup and protocol are complicated and contain multiple components, including preparation of the clot, plasma and rt-PA mixture, histotripsy, ultrasound imaging guidance and monitoring, treatment delivery, and post treatment evaluation. The authors provide a thorough and detailed description that will enable other groups to replicate their study.

Major Concerns:

None.

We thank the reviewer for positive reviews and comments. Below are the explanations for the reviewer's comments:

1. *Page 3, line 68-70 - "It is hypothesized that two primary mechanisms …… and 2) hemolysis of red blood cells within the clot." Does histotripsy only break down red blood cells? How about other contents in the clot?*

   Debris from histotripsy insonation is predominately subcellular in size[1-3]. It is therefore likely that other formed clot elements are disintegrated by histotripsy bubble activity. Red blood cells are the primary contribution to the mass of the clot specimen described in the article[1], and their degradation are thus the primary marker associated with ablation of the clot. The text has been edited in line 70 of page 2 to include this information as follows

   The bulk of the clot mass is comprised of red blood cells[1], and therefore tracking erythrocyte degradation is a good surrogate for ablation of the sample. Other formed clot elements are also likely disintegrated under histotripsy bubble activity, but are not considered in this study.

2. *Page 4, line 95 - "1.4 Store the pipettes for a minimum of three days at 4 °C to allow for retraction for clots." Does the surface of the pipette need to be hydrophilic for the clot retraction to occur? Do you expect to see serum to extract out of the clot after a few days?*

   The reviewer is correct in stating that the pipettes need to be hydrophilic[4], such as the borosilicate pipettes highlighted in this protocol (see Table of Materials). As the clots retract, serum is observed in the pipettes. The protocol has been modified to include this information in step 1.1 and 1.4 (lines 96-106 of page 3), as follows

   1.1. Prepare borosilicate Pasteur pipette for storing the blood (see Table of Materials for specifications of the pipette). Borosilicate tubes are used because of the hydrophilic nature of the material which promotes platelet activation and clot retraction[4]. Seal the tip of the pipette via heating over a Bunsen burner.

   1.4. Store the pipettes for a minimum of three days at 4 °C to allow for retraction for clots [5]. As the clots retract, serum will be observed to accumulate within the pipette. The rt-PA response of clots remains stable for 2 weeks following formation[5].

3. *Page 6, line 152 - "4.5 Connect the imaging array to an ultrasound scanning system (e.g. Verasonics)." What needs to be done to align that ultrasound imaging probe and the histotripsy transducer such that the ultrasound imaging array is viewing the histotripsy focus? How to mark the histotripsy focus on ultrasound imaging?*

   The text was modified to highlight that the imaging array position should be adjusted until a bubble cloud is visualized via ultrasound imaging to ensure proper alignment of the array relative to the transducer. We have also adjusted the text to indicate that the focal location can either be recorded offline, or via cursors as available with the imaging platform: The protocol has been modified for steps 4.10-4.12 (lines 194– 207 of page 6) to include this information as follows

   4.10. Using the real-time imaging of step 4.7, adjust the position of the imaging array inside the confocal transducer opening until the bubble cloud is located approximately at the center of the image window. The bubble cloud is the region of hyperechoic pixels in the imaging plane (Figure 3). Tighten the screws to hold the imaging array firmly in the transducer opening.

NOTE: If the array is aligned properly, the azimuthal position of the bubble cloud should be approximately at 0 mm. The imaging array may project slightly from the inner surface of the therapy source, and therefore the range position of the bubble cloud may differ from the focal length of the source.

4.11. Identify the bubble cloud location in the imaging plane. Assign the focus of the histotripsy source as the center of the bubble cloud (Figure 3).

4.12. Record the detected focal location (step 4.11) in the imaging window (Figure 3). A possible way to mark the focal position is placing a cursor to note the location in the imaging window, if available with the imaging platform.

4. *Page 7, line 209 - "6.1 At a rate of 10 mL/min, draw the plasma into the flow channel from the reservoir via the pump until the plasma fills the model vessel." Why set the flow rate to be 10 mL/min? What is the range of venous flow rate in the condition of partial to complete obstruction?*

Step 6.1 instructs users to ensure the lumen is filled prior to application of the histotripsy pulse. The infusion rate is not critical in this step. The text here has been revised (line 237 of page 7):

6.1 Draw plasma into the flow channel from the reservoir via the syringe pump until the model vessel is filled. Ensure that the flow rate does not disturb the clot but fills the model vessel efficiently.

When histotripsy pulses are applied starting in step 7.2.1, the flow rate should be fixed at 0.65 mL/min. This flow rate is consistent with a near total iliofemoral occlusion[1,6]. The protocol in step 7.2.1 (line 279 of page 8) is revised to clear this information in for the readers, as follows

7.2.1. Run the pump connected to the syringe at 0.65 mL/min and wait for meniscus of the plasma to move. This flow rate mimics a near total occlusion of the iliofemoral vasculature[1,6].

5. *Page 12, line 389 - "The operating parameters of the transducer should be chosen to avoid off target effects while maximizing mechanical clot disruption." Using the given parameters, how large was the flow channel created? The flow channel seems to be too small to be clinically relevant. What can be done to increase the flow channel size?*

   Mass loss, not restoration of flow or estimation of flow channel area created within the clot, was a primary metric of treatment efficacy in this protocol. With an appropriate choice of insonation parameters, a 94% reduction in clot mass was achieved. Employing the protocol outline here, an insonation scheme for total clot removal can be devised to ensure total restoration of flow. The following text was added in line 439 of page 13 to highlight this:

   In this protocol, mass loss was considered a primary metric of treatment efficacy. Increases in mass loss has been observed as the peak negative pressure or the duration of the histotripsy pulse are increased[1,7], with a maximum observed mass loss of 94%. The presence of residual clot for investigated treatment arms facilitates comparison of therapeutic efficacy. However, insonation schemes to ensure total removal of the thrombus can also be devised.

   The following text was added in line 416 of page 12 to highlight this (Figure 6 caption):
   Note that the degree of clot disruption achieved here would be reduced compared to insonation schemes with longer pulse duration.

   The following text was added in line 480 of page 14 to highlight that flow (clinical endpoint) was not considered in this study:

   Restoration of flow is also the primary clinical endpoint for treatment efficacy, whereas mass loss was a primary metric for treatment efficacy in the protocol described here.

6. *Page 13, line 414 - It was stated that real-time passive cavitation detection overlaid on ultrasound B-mode images was achieved. What was the frame rate?*

   The reference to "real-time display" in this section refers to standard B-mode imaging for pre-treatment planning, not real-time processing of passive cavitation imaging. We have clarified that passive cavitation imaging was analyzed post hoc with the following sentence in line 466 of page 13 as follows:

   The imaging system should be programmed to trigger on based on the known time of flight of the histotripsy pulse from the source to the focal zone, to ensure collection of passive cavitation imaging data throughout the insonation. These signals should then be processed post hoc as discussed in steps 7.2.3 and 9 of the protocol.

Reviewer #2 (Comments to the Author):

Manuscript Summary:

The manuscript presents the details of a convenient in vitro platform for testing different histotripsy approaches to the intravascular clot lysis in DVT (deep vein thrombosis). Given the recent successful results achieved in histotripsy thrombolysis by the authors and other groups, this information will be useful to the thrombolysis community.

Major Concerns:
None.

We thank the reviewer for a positive review and insightful comments. Below are the explanations for the reviewer's comments:

1. *In item 2.3: "...model vessel with material properties representative of an iliofemoral vein..." which properties are the authors referring to? Speed of sound? Density? Flexibility? Wall thickness? While the specific material used here is listed in the Table, it would be useful to add which material properties are important to look for, in case the specified material is for some reason unavailable. It could be added either here or in the discussion (or both).*
   The acoustic impedance and geometry of the iliofemoral vein are modeled by the model vessel proposed in this study, as highlighted in the discussion (line 445 of page 13):
   The acoustic impedance (approximately 1.58 MRayl[8,9]) and the geometrical properties (0.6-1.2 cm in diameter[10]) of the model vessel should be representative of the iliofemoral venous vasculature (see Table of Materials for details). Polydimethylsiloxane and polyurethane are some of the materials suitable to model the venous system based on their acousto-mechanical properties.

1 Bollen, V. *et al.* In Vitro Thrombolytic Efficacy of Single- and Five-Cycle Histotripsy Pulses and rt-PA. *Ultrasound in medicine & biology.* **46** (2), 336-349, (2020).

2 Bader, K. B. *et al.* Efficacy of histotripsy combined with rt-PA in vitro. *Phys Med Biol.* **61** (14), 5253-5274, (2016).

3 Xu, Z. *et al.* Size measurement of tissue debris particles generated from pulsed ultrasound cavitational therapy-histotripsy. *Ultrasound in medicine & biology.* **35** (2), 245-255, (2009).

4 Sutton, J. T., Ivancevich, N. M., Perrin, S. R., Jr., Vela, D. C. & Holland, C. K. Clot retraction affects the extent of ultrasound-enhanced thrombolysis in an ex vivo porcine thrombosis model. *Ultrasound in medicine & biology.* **39** (5), 813-824, (2013).

5 Holland, C. K., Vaidya, S. S., Datta, S., Coussios, C.-C. & Shaw, G. J. Ultrasound-enhanced tissue plasminogen activator thrombolysis in an in vitro porcine clot model. *Thrombosis research.* **121** (5), 663-673, (2008).

6 Jensen, C. T. *et al.* Qualitative slow blood flow in lower extremity deep veins on doppler sonography: quantitative assessment and preliminary evaluation of correlation with subsequent deep venous thrombosis development in a tertiary care oncology center. *Journal of Ultrasound in Medicine.* **36** (9), 1867-1874, (2017).

7 Hendley, S. A., Paul, J. D. & Bader, K. B. in *Joint AAPM | COMP Virtual Meeting.* (American Association of Physics in Medicine).

8 Goss, S. A., Johnston, R. L. & Dunn, F. Comprehensive compilation of empirical ultrasonic properties of mammalian tissues. *The Journal of the Acoustical Society of America.* **64** (2), 423-457, (1978).

9 Duck, F. A. in *Physical Properties of Tissues* https://doi.org/10.1016/B978-0-12-222800-1.50009-7 (ed Francis A. Duck) 137-165 (Academic Press, 1990).

10 De Sensi, F. *et al.* Predictors of Successful Ultrasound Guided Femoral Vein Cannulation in Electrophysiological Procedures. *Journal of atrial fibrillation.* **11** (3), 2083-2083, (2018).